Int. J. Electrochem. Sci., 8 **(2013)** 9133 - 9148

International Journal of
ELECTROCHEMICAL
SCIENCE
www.electrochemsci.org

Spectral, Electrochemical and Antimicrobial Activity of Thiophene-cyclodiphosph(V)azane and Its Mn(II), Fe(III), Fe(II), Co(II), Ni(II), Cu(II), Zn(II), Cd(II), and UO_2(II) Complexes

Salwa A. H. Albohy

Department of Chemistry, Faculty of Science, Al-Azhar University (Girls), Nasr City, Cairo, Egypt
*E-mail: salwaalbohy@yahoo.com

Received: 19 April 2013 / *Accepted:* 5 June 2013 / *Published:* 1 July 2013

The ligand, 1,3-di(o-chlorophenyl)-2,4-bis(2-amino-5,6,7,8-tetrahydro-4H-cyclohepta[b]-thiophene-3-carbonitrile)-2,2,4,4-tetrachlorocyclodiphosph-(V)azane (H_2L) and its complexes with Mn(II), Fe(III), Fe(II), Co(II), Ni(II), Cu(II), Zn(II), Cd(II), and UO_2(II) ions were prepared and characterized by microanalytical, IR, molar conductance, thermal analyses, UV-Vis, ^{1}H-, ^{13}C and ^{31}P- NMR, ESR, solid reflectance, Mössbauer, XRD, magnetic susceptibility measurements and biological activity. The ligand acts in a tetrahedral manner forming 2:1 metal to ligand ratio. The UV-Vis, solid reflectance, and magnetic-moment data have shown that the ligand is coordinated to the metal ions in an octahedral manner. The redox behavior of complexes was investigated by cyclic voltammetry. The antimicrobial activities of the H_2L and their alkaline metal complexes were evaluated.

Keywords: cyclodiphosph(V)azane; electronic; IR; magnetic moment; DNA cleavage

1. INTRODUCTION

In recent years, the structural feature of four-membered N_2P_2 ring compounds in which the coordination number of *P* varies from three to five have attached considerable attention[1,2]. Heterocycles with P−C, P−N, P−O, and P−S bonds, in addition to their great biochemical and commercial importance[3,4], play a major role in some substitution mechanisms as intermediates or as transition states[3,4]. Also, some *P*-containing heterocycles had been found to be potentially carcinostatics[3] among other pharmacological activities. The introduction of tervalent *P* centers in the ring enhanced the versatility of the heterocycles in complexing with both hard and soft metals. Since

the tervalent *P* centers could stabilize transition metals in low oxidation states, such complexes could be potential homogeneous or phase-transfer catalysts in various organic transformations[3].

In a continuation of our earlier studies on the coordination chemistry of Schiff base ligand, herein we report synthesis and structural studies of Mn(II), Fe(III), Fe(II), Co(II), Ni(II), Cu(II), Zn(II), Cd(II), and UO_2(II) with a potentially bidentate aminocyclodiphosph(V)azane, 1,3-di(*o*-chlorophenyl)-2,4-bis(2-amino-5,6,7,8-tetrahydro-4H-cyclohepta[b]-thiophene-3-carbonitrile)-2,2,4,4-tetrachlorocyclodiphosph-(V)azane (H_2L) (see Scheme 1).

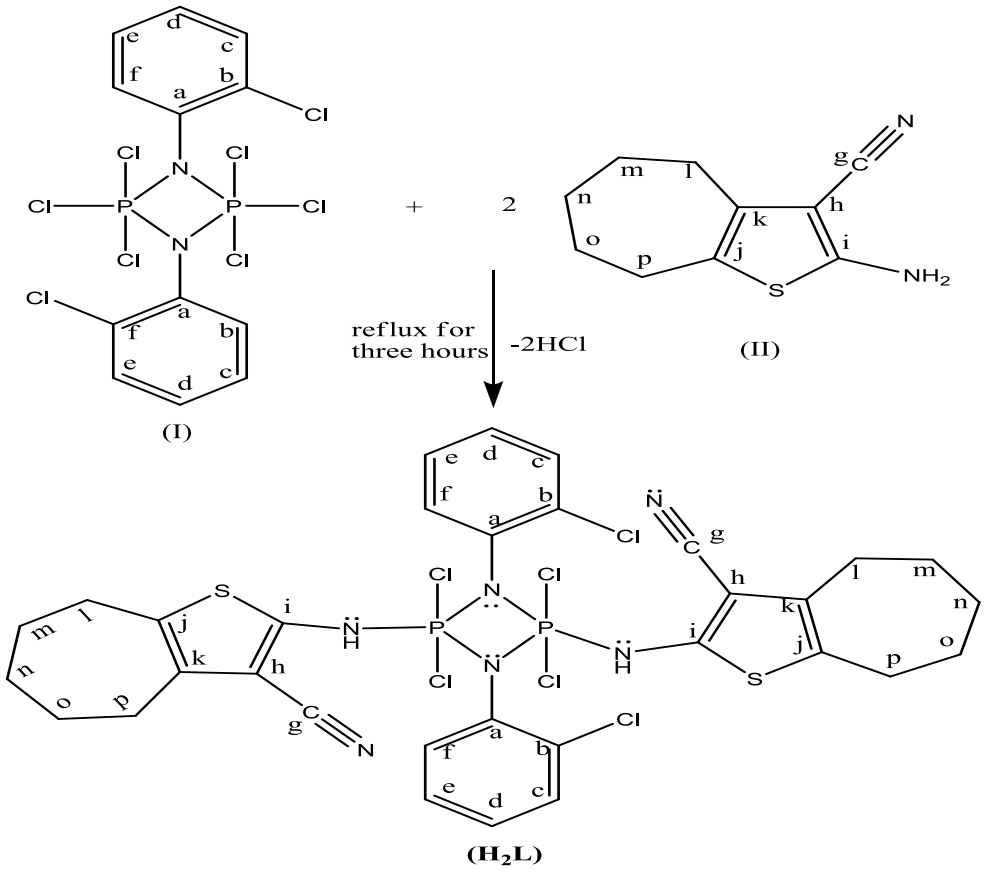

Scheme 1

2. EXPERIMENTAL

2.1. Preparation of the ligand (H_2L)

The solid of 2–amino–5,6,7,8–tetrahydro–4H–cyclohepta[b]thiophene–3-carbonitrile **(II)** (1.92 gm; 0.01 mmol) was added in small portions to a well stirred solution of the hexachlorocyclodiphosph(V)azane **(I)** (2.285 gm; 0.005 mmole) in 100 ml acetonitrile over a half–hour period. After the complete addition, the reaction mixture was heated under reflux for 3 hrs with continuous stirring. After completion of the reaction (HCl gas ceased to evolve) the reaction mixture was filtered while hot and the filtrate was left to cool at room temperature. The obtained solid

was filtered washed several times with acetonitril, diethylether and dried under vaccuo to give the corresponding cyclodiphosph(V)azane thiophene derivatives **H_2L** the data obtained are listed in Table 1.

Table 1. Elemental analyses, yields, colours, and melting points of ligand (H_2L) and its corresponding metal complexes.

No.	Mol. Formula (M. wt.) [M.p. °C]	(Yield%) Colour	Elemental analyses Found (Calc.), %							Λ_m (Ω^{-1} mo^{-1}cm^2)
			C	H	N	P	Cl	S	M	
H_2L	$C_{32}H_{30}Cl_6N_6P_2S_2$ (837.42) [200-202]	(88) Yellow	50.00 (45.90)	4.20 (3.61)	10.93 (10.04)	8.04 (7.40)	18.44 (25.40)	8.34 (7.66)	--	--
1	$C_{40}H_{50}Cl_6Mn_2N_6O_{12}P_2S_2$ (1255.53) [>300]	(77) Rose	38.26 (38.26)	4.00 (4.01)	6.67 (6.69)	4.92 (4.93)	16.86 (16.94)	5.12 (5.11)	8.75 (8.75)	7
2	$C_{32}H_{38}Cl_{12}Fe_2N_6O_4P_2S_2$ (1233.89) [>300]	(62) Brown	31.16 (31.15)	3.14 (3.10)	6.26 (6.81)	5.38 (5.32)	34.41 (34.48)	5.25 (5.20)	9.00 (9.05)	135
3	$C_{32}H_{38}Cl_6Fe_2N_6O_{12}P_2S_4$ (1213.29) [>300]	(82) Brown	31.48 (31.68)	3.10 (3.16)	6.89 (6.93)	5.38 (5.41)	17.38 (17.53)	10.16 (10.57)	9.20 (9.21)	8
4	$C_{40}H_{50}Cl_6Co_2N_6O_{12}P_2S_2$ (1263.52) [>300]	(85) Brown	38.02 (38.02)	3.99 (3.99)	7.04 (7.03)	5.11 (5.11)	11.85 (16.84)	5.34 (5.37)	9.30 (9.33)	7
5	$C_{40}H_{50}Cl_6N_6Ni_2O_{12}P_2S_2$ (1263.04) [>300]	(85) Green	38.04 (38.04)	3.99 (3.99)	6.65 (6.65)	4.90 (4.90)	16.82 (16.84)	5.08 (5.08)	9.29 (9.29)	12
6	$C_{40}H_{50}Cl_6Cu_2N_6O_{12}P_2S_2$ (1272.75) [>300]	(83) Green	37.92 (37.75)	4.24 (3.96)	6.95 (6.60)	5.12 (4.87)	16.81 (16.71)	5.00 (5.08)	10.00 (9.99)	9
7	$C_{40}H_{50}Cl_6N_6O_{12}P_2S_2Zn_2$ (1276.47) [>300]	(68) Yellow	37.53 (37.64)	3.62 (3.95)	6.90 (6.58)	5.10 (4.85)	16.10 (16.66)	5.00 (5.04)	10.24 (10.25)	10
8	$C_{32}H_{38}Cd_2Cl_{10}N_6O_4P_2S_2$ (1276.11) [>300]	(78) Yellow	30.12 (30.12)	3.00 (3.00)	6.94 (6.59)	5.10 (4.85)	27.78 (27.78)	5.17 (5.03)	17.50 (17.62)	8
9	$C_28H_{32}Cl_6N_10O_{20}P_2S_4U_2$ (1708) [>300]	(77) Yellow	19.69 (19.69)	1.95 (1.89)	8.54 (8.20)	3.75 3.63)	12.46 (12.46)	7.82 (7.51)	27.88 (27.88)	137

2.2. Preparation of complexes (1-9)

A solution of the metal salts (0.002 mole) in 50mL dry ethanol was added dropwise to a solution of thiohene–cyclodiphosph(V)azane (0.001mole) in 100 mL absolute ethanol in a 2:1 metal to ligand molar ratio at room temperature with continuous stirring. After complete addition of the metal salt solution, the reaction mixture was heated under reflux for about three hours under dry conditions. The complexes obtained were washed with dry ethanol then with dry diethylether and dried in vacuo. The products obtained give elemental analyses consistent with the proposed formula.

2.3. Methods

Elemental analyses were determined at the Microanalytical Unit of Cairo University (Egypt) using CHNS-932 (LECO) Vario EL elemental analyzers. Metal contents were determined by titration against standard EDTA after complete decomposition of the complexes with aqua regia in a Kjeldahl flask several times. Infrared spectra were recorded in the solid state on a Mattson 5000 FTIR spectrometer using KBr disc technique. The absorbances of solutions were measured in the UV/VIS range (200–800 nm) using Unicam spectrophotometer model UV 2-100 and 1 cm matched quartz cells. ^{1}H and ^{13}C NMR spectra were taken on a Varian Mercury 300MHz Em-360-60 MHz instrument. TMS was used as internal standered and deuterated dimethyl sulfoxide as solvent. ^{31}P NMR spectra were run, relative to external H_3PO_4 (85%), with a varian FT-80 spectrometer at 36.5MHz. The mass spectra were performed by a Shimadzu-Ge-MS-Qp 100 EX mass spectrometer using the direct inletsystem. Magnetic measurements were recorded by the Gouy method at room temperature using a magnetic susceptibility balance (Johnson Mathey), Alfa product, Model No. (MK). Diamagnetic corrections were calculated from Pascal's constants. The conductometric measurements in solutions were carried out using conductivity TDS model 72. Mössbauer measurements were performed in the Physics Department, Faculty of Science, Al-Azhar University, at room temperature in a transmission geometry employing ^{57}Co as a radioactive source. The spectra were analyzed using a computer program based on Lorentzian distribution. The isomer shifts were expressed relative to a metallic iron absorber.The thermogravimetric analyses (TGA) were recorded on a Shimadzu TGA-50H. TGA was carried out in a dynamic nitrogen atmosphere (20mL min^{-1}) at a heating rate of 10 °C min^{-1}.ESR spectra recorded on the Bruker, Model: EMX, X-band spectrometer. The magnetic field was calibrated with a 2, 2-diphenyl-1-picrylhydrazyl sample. Electrospray mass spectral data were obtained with 5×10^{-4} M solutions (MeOH or CH_2Cl_2) by flow injection into a Hewlett–Packard 1100 series MSD. The carrier solvent was 49% MeOH/49% H_2O/2% formic acid or 98% CH_2Cl_2/2% formic acid. Electrospray ionization conditions were as follows: nitrogen drying gas flow 10.0 l min^{-1}; nebulizer pressure, 40 psig; drying gas temperature 350 °C; capillary voltage, 4 kV. The capillary exit voltage was varied from 0 to 150 V.

2.4. Biological activity

About 0.5mL spore suspension (10^{-6} to 10^{-7} spore/mL) of each of the investigated organisms was added to a sterile agar medium just before solidification, then poured into sterile Petri dishes (9 cm in diameter) and left to solidify. Using sterile cork borer (6mm in diameter), three holes (wells) were made in each dish, then 0.1mL of the tested compounds dissolved in DMF (100 (g/mL) were poured into these holes. Finally, the dishes were incubated at 37 °C for 48 h where clear or inhibition zones were detected around each hole. About 0.1mL DMF alone was used as a control under the same condition for each organism and by subtracting the diameter of inhibition zone resulting with DMF from that obtained in each case, both antimicrobial activities can be calculated as a mean of three replicates [5, 6].

3. RESULTS AND DISCUSSION

The purity of the ligand (H_2L) 98.44% has been checked by HPLC. The EI-mass spectrum of the ligand (H_2L) shows a maxima peak at 768 u, corresponding to the macrocyclic moiety (($C_{32}H_{30}Cl_6N_6P_2S_2$), calculated atomic mass 837 u) and a number of peaks at 14, 29, 48, 78, 85, 125, 198, 202 and 346 u, attributable to different fragments of the ligand (Fig. 1). In the IR spectra of the complexes the absence of the bands characteristic for primary ammines (~3400 cm^{-1}) suggests that the complete reaction had occurred. The appearance of a new, strong intensity, band in the region 2600 cm^{-1}, attributed to the characteristic stretching frequencies of the phospho imino linkage *v*(P-NH), provides strong evidence in favour of the formation of thiophene-cyclodiphosph(V)azane product. Another IR spectral peak in the region 409–461 cm^{-1} attributed to *v*(M–N). The shifting of *v*(P-NH) and *v*(M–N) bands, in lower side, provides strong evidence for the involvement of nitrogen in coordination. Hence we conclude out that the ligand is bidentate coordinating through two nitrogen atoms. ^{1}H, ^{13}C and ^{31}P NMR (DMSO-d_6), showed the characteristic proton signals, which are listed in Table 2. The UV spectrum of the ligand in DMF solvent showed absorption band at 273 nm, which are due to the electron delocalization within the four membered ring of the dimeric structure for the ligand.

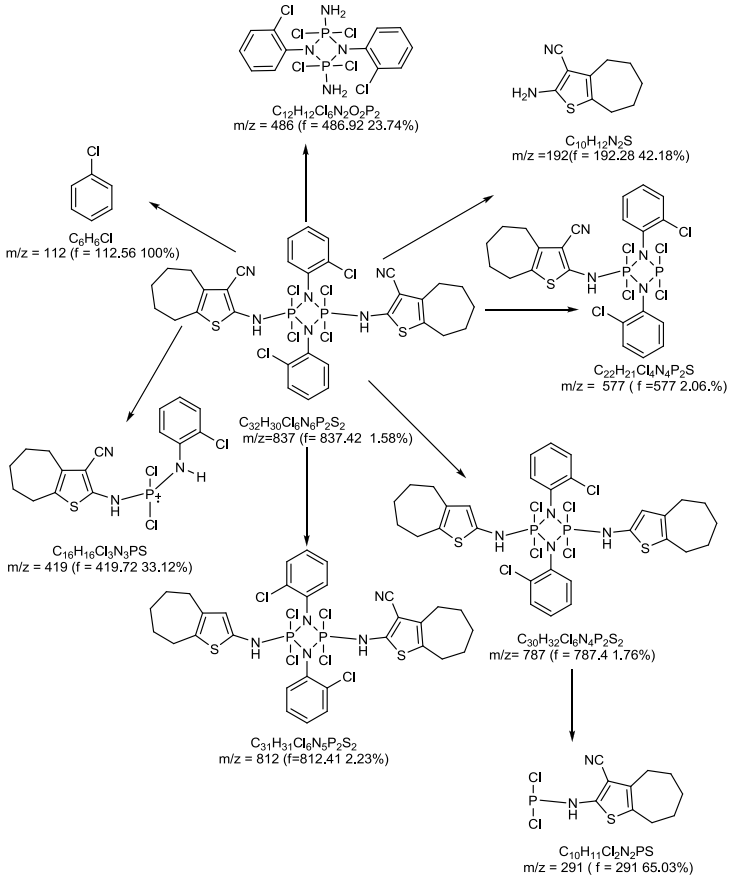

Figure 1. Possible fragmentation pathways of H_2L ligand.

3.2. Metal Complexes

The analytical data of ligand and its complexes with their physical properties are given in Table 1. The elemental analyses of the complexes were consistent with the $[M_2(H_2L)(OAc)_4(H_2O)_4]$, $[Cd_2(H_2L)(Cl)_2(H_2O)_2]$, $[Fe_2(H_2L)(Cl)_2(H_2O)_4]$ 2Cl, $[Fe_2(H_2L)(SO_4)_2(H_2O)_4]$, and $[(UO_2)_2(H_2L)(NO_3)_2(H_2O)_2].2NO_3.2H_2O$ compositions, where M= Mn(II), Co(II), Ni(II), Cu(II) and Zn(II), H_2L ligand,. The molar conductivity value of the complexes 1&3-8 in DMSO indicates that the complexes are nonelectrolytes [7], while the molar conductance data of the complexes 2, 9

2,9 corresponds to their 1:2 electrolyte nature by showing the molar conductance value in the range 135 and 137 Ω^{-1} cm^2 mol^{-1} [7], respectively.

3.3. IR spectra of the complexes

The nitrato complexes show IR bands at 1420 –1448 (ν_5), 1317–1321 (ν_1) and 1023–1077 cm^{-1} (ν_2). The ν_5 and ν_1 NO_3 stretching vibrations are separated by 101–131cm^{-1} which suggests the unidentate coordination nature of NO_3^- ions [8–10]. The acetato complexes show bands at 1425–1429 (A_1) and 620–624 cm^{-1} (B_2) due to coordinated acetate anion [11]. The bands at 328–329cm^{-1} are present in chloro complexes which are attributed to the _(M–Cl) [12]. In the IR spectra of all complexes, the bands at 815–816 and 612–618cm^{-1} are present which are characteristic bands of $\rho r(H_2O)$ and $\rho_w(H_2O)$. These bands are assigned to the coordinated water molecule [13,14]. The ν(U=O) vibration in the uranyl complex (9) is observed as expected as a very strong band at 927 cm^{-1} is a good agreement with those known for many dioxouranium (IV) complexes[15].

3.4. Electronic spectra and magnetic properties

The UV–vis spectra of the ligand and the complexes were recorded in DMF solution in the wavelength range from 200to 800 nm. The spectra showed a sharp and intense band in the 270 nm region, which is characteristic for phosphazo four membered rings of the ligands. The blue or red shifts of the band in the region (267–276 nm) with respect to the ligand depend on the type of metal ions coordinated to the ligand.

The diffuse reflectance spectrum of Mn(II) complex **(1)** shows three bands at 15,660, 22,235 and 26,435 cm^{-1} assignable to $^4T_{1g}\rightarrow{}^6A_{1g}$, $^4T_{2g}$ (G)$\rightarrow{}^6A_{1g}$ and $^4T_{1g}$ (D)$\rightarrow{}^6A_{1g}$ transitions, respectively[16]. The magnetic moment value is 5.07 μB which indicates the presence of Mn(II) complex in octahedral structure.

It is observed from the diffuse reflectance spectra of the Fe(III) complex **(2)** that they exhibit a band at 21,165–21,185 cm^{-1} which may be assigned to the $^6A_1g\rightarrow T_2g$ transition in octahedral geometry [16]. The spectra also show a spitted bands at 14,935–15,695 and 17,560–18,365 cm^{-1} which assigned to the $^6A_1g\rightarrow{}^5T_1g$ transition. The observed magnetic moment of the Fe(III) complex is 5.01 μB for H_2L ligand, respectively, which confirm the octahedral geometry[17]. The bands observed at 29,165 and 24,960–26,130 cm^{-1} can be attributed to ligand-to-metal charge transfer band for the Mn(II) and Fe(III) complexes, respectively [17].

The diffuse reflectance spectrum of Fe(II) complex **(3)** displays two absorption bands at 15,175 cm^{-1} and 22,230cm^{-1} which are assigned to $^5T_2g \rightarrow {}^5E_g$ transitions [18]. Also, the band at 25,650 cm^{-1} is assigned to L→M charge transfer[18]. The observed magnetic moment of 4.93 B.M. is consistent with an octahedral geometry[18].

The electronic spectrum of the Co(II) complex **(4)** displays two bands at 15,315 cm^{-1} and 17,480 cm^{-1} assigned to the $^4T_1g \rightarrow {}^4T_1g$ (*P*) and $^4T_1g \rightarrow {}^4T_2g$ (*F*) transitions, respectively, which arise due to ligand field transition of the pseudo octahedral component of the Co(II) complex. The observed magnetic moment value is μ_{eff} = 3.85 B.M. at room temperature which confirms the octahedral structure of this cobalt complex[18]. The band observed at 22,655 cm^{-1} refers to L→M CT band.

The solid reflectance spectrum of the Ni(II) complex **(5)** shows bands at 23,235, 17,465 and 18,925 cm^{-1}, suggesting the existence of $^3A_2g \rightarrow {}^3T_1g$ (*P*), $^3A_2g \rightarrow {}^3T_1g$ (*F*) and $^3A_2g \rightarrow {}^3T_2g$ transitions, respectively, with an octahedral spatial configuration. The observed magnetic moment of the complex is 2.86 B.M., which confirms the octahedral structure of this complex[19].

The solid reflectance spectrum of the Cu(II) complex **(6)** gave a band at 16,825 cm^{-1}, which may be assigned to $^2Eg \rightarrow {}^2T_2g$[20]. The observed magnetic moment of the Cu(II) complex is 1.84 B.M., which confirms the octahedral structure of this complex. The band observed at 22,945 cm^{-1} refers to L→MCT band[20].

The Zn(II) and Cd(II) complexes**(7,8)** are diamagnetic as expected and its geometry is most probably octahedral similar to the Mn(II), Fe(III), Fe(II), Co(II), Ni(II) and Cu(II)complexes of the ligand (**H_2L**)[21].

The electronic spectrum of the yellow UO_2(II) complex **(9)** arises from the electronic transition of metal→ligand charge transfer. This is an allowed transition and produces a broad, intense absorption band at 20,635 cm^{-1} for complex **(9),** tailing into the visible region. This produces the intense yellow color, where the UO_2(II) complexes are diamagnetic as expected [22].

3.5. ^1H, ^{13}C and ^{31}P NMR spectra of the Zn(II), Cd(II) and UO_2(II) complexes

Table 2. The ^1H, ^{13}C and ^{31}P NMR data (as ppm) for the ligand and its Zn(II), Cd(II), and UO_2(II) using DMSO as solvent

Compd.	NMR δ (ppm)																		
	$^1H(^{13}C)$																		^{31}P
	CH (aromatic ring)						C≡N	Thiophene ring				CH_2 (Cycloheptane)					OCOCH$_3$		
	a	b	c	d	e	f	g	h	i	j	k	l	m	n	o	p	q	r	
Ligand	-- (112.8)	7.20 (113.0)	7.38 (123.8)	7.53 (136.6)	7.64 (149.5)	7.70 (152.3)	7.20 (113.64)	-- (125.2)	-- (128.6)	-- (144.8)	-- (163.7)	2,2 (24.5)	2.26 (24.6)	2.34 (26.8)	2.45 (27.4)	2.53 (28.4)	--	--	14
Zn(II)	-- (113.6)	7.20 (117.2)	7.38 (124.3)	7.53 (137.6)	7.64 (149.9)	7.70 (153.6)	7.20 (113.6)	-- (124.3)	-- (127.4)	-- (143.5)	-- (163.8)	2,23 (113.6)	2.23 (24.2)	2.32 (26.5)	2.42 (27.3)	2.53 (28.8)	2.52 (30.4)	3.31 (31.2)	25
Cd(II)	-- (113.4)	7.20 (117.5)	7.38 (124.4)	7.53 (138.6)	7.64 (150.4)	7.70 (154.8)	7.20 (113.6)	-- (124.5)	-- (127.3)	-- (143.7)	-- (164.6)	2,23 (113.6)	2.22 (24.2)	2.3 (26.4)	2.41 (27.3)	2.57 (28.3)	2.65 (30.7)	3.43 (32.5)	25
UO_2(II)	-- (113.2)	7.20 (117.5)	7.38 (124.6)	7.53 (138.3)	7.64 (150.5)	7.70 (154.4)	7.20 (113.6)	-- (124.1)	-- (128.8)	-- (143.4)	-- (165.3)	2,20 (113.6)	2.22 (24.3)	2.33 (26.4)	2.44 (27.2)	2.57 (28.3)	2.72 (30.2)	3.54 (32.3)	25

A survey of literature revealed that the NMR spectroscopy has been proved useful in establishing the nature and structure of ligand as well as their Zn(II), Cd(II) and UO_2(II) complexes in solutions. The ^{1}H NMR spectrum of ligand **H_2L** was recorded in dimethylsulfoxide (DMSO-d_6) solution using TMS (0 ppm) as internal standard. ^{1}H, ^{13}C and ^{31}P NMR (DMSO-d_6), showed the characteristic proton signals, which are listed in Table 2.

3.6. Mössbauer Spectroscopy

The Mössbauer spectra were measured at room temperature for iron complexes. The spectra revealed the presence of Fe ions in $[(FeCl_2)_2(H_2L)\text{-}(H_2O)_4]2Cl$, and $[FeSO_4)(H_2L)(H_2O)_4]$ in ferric and ferrous oxidation state respectively in octahedral coordination [23]. The Mössbauer parameters are listed in Table 3 and Fig. 2.

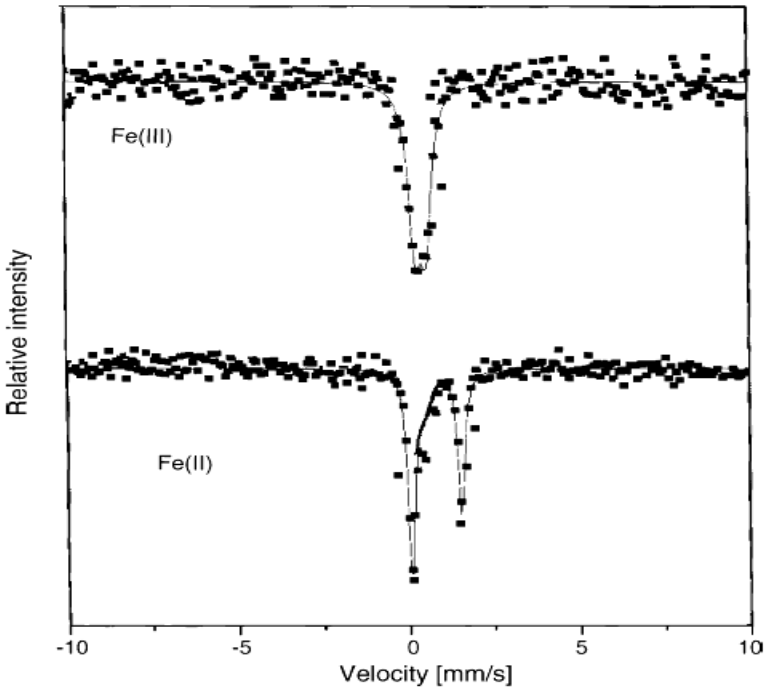

Figure 2. Mössbauer spectra of the iron complexes.

Table 3. Mössbauer parameters for iron complexes of the H_2L ligand.

Complex	Isomer shift (IS) (mm/s)	Quadrupole splitting(QS) (mm/s)
$[(FeCl_2)_2H_2L(H_2O)_4].2Cl$	0.47	0.75
$[FeSO_4)_2H_2L(H_2O)_4]$	1.8	4.4

3.7. ESR spectrum of Cu(II) complex

The EPR spectrum of Co(II) complex was recorded as polycrystalline sample. No EPR signal was observed at room temperature because the rapid spin lattice relaxation of Co(II) broadens the lines

at higher temperature. It shows a very broad signal at liquid nitrogen temperature. The deviation of '*g*' values from the free electron value (2.0023) may be due to angular momentum contribution in the complexes [24].

The EPR spectrum of the copper(II) complex shows two lines having $g_{\parallel}$ value at 2.11 and $g_{\perp}$ at 2.04. $g_{\parallel}$ value being less than 2.3, witnesses more covalency in metal–ligand interaction [25]. Further it is noteworthy that the relation $g_{\parallel} > g_{\perp} > g_e$ (2.0029) is typical of axially symmetric d^9 Cu^{II} ion having one unpaired electron in $d_{x^2-y^2}$ orbital [26-29].

3.8. Thermal Studies (TGA and DrTG)

Table 4. Thermogravimetric data of **H_2L** metal complexes

Complex	TG rang (ºC)	DTG max (ºC)	n[a]	%Found (Calcd.) Mass loss	%Found (Calcd.) Total mass loss	Assignment of the removed species	Metallic Residue Found (calcd. %)
$[FeSO_4)_2H_2L(H_2O)_4)]$	30–250	70, 170	2	6.26 (6.29)	73.38 (73.44)	Loss of $4H_2O$	$2Fe_2SO_4$
$[(CdCl_2)_2H_2L(H_2O)_4]$	250–100	270, 670	2	67.12 (67.15)		Loss of ligand	
	50-360	320	1	61.49 (61.57)	78.66 (78.87)	Loss of $4HCl,O_2$ and $C_{26}H_{26}Cl_4N_2P_2$	2CdS
	360-700	480	1	17.17 (17.30)		Loss of $C_2H_2N_4$	
$[UO_2(NO_3)_2H_2L(H_2O)_2].NO_3.2H_2O$	30-135	51.16	1	2.14 (2.19)	51.24 (51.34)	Loss of $2H_2O$	$2UO_2(NO_3)_2$
	135-1000	102.6, 182.8, 243.2	3	49.10 (49.15)		Loss of $2H_2O$ and ligand	

In the present investigation, heating rates were suitably controlled at 10 °C min^{-1} under nitrogen atmosphere and the weight loss was measured from the ambient temperature up to1000 °C. The data are listed in Table 4. The weight losses for each chelate were calculated within the corresponding temperature ranges. The different thermodynamic parameters are listed in Table 5. The thermodynamic activation parameters of decomposition processes of dehydrated complexes namely activation energy (E^*), enthalpy (ΔH^*), entropy (ΔS^*) and Gibbs free energy change of the decomposition (ΔG^*) were evaluated graphically by employing the Coats–Red fern relation [30]. The entropy of activation (ΔS^*), enthalpy of activation (ΔH^*) and the free energy change of activation (ΔG^*) were calculated using the following equations:

$$\Delta S^* = 2.303\ [\log(Ah/Kt)]\ R \quad (1)$$

$$\Delta H^* = E^* - RT \quad (2)$$

$$\Delta G^* = \Delta H^* - T\Delta S^* \quad (3)$$

The data are summarized in Table 5. The activation energies of decomposition were found to be in the range 22.95–243.4 kJ mol^{-1}. The high values of the activation energies reflect the thermal

stability of the complexes. The entropy of activation was found to have negative values in all the complexes which indicate that the decomposition reactions proceed with a lower rate than the normal ones. According to the kinetic data obtained from DTG curves, all the complexes have negative entropy, which indicates that activated complexes have more-ordered systems than reactants [31].

Table 5. Thermodynamic data of the thermal decomposition of H_2L the complexes

Complex	TG rang (ºC)	E* (kJ mol^{-1})	A (S^{-1})	ΔS* ($kJmol^{-1}$)	ΔH*(kJ mol^{-1})	ΔG* (kJ mol^{-1})
$[FeSO_4)_2H_2L(H_2O)_4)]$	30–110	53.25	2.87×10^{8}	−34.65	45.65	37.22
	140–230	82.37	4.55×10^{12}	−62.66	97.16	76.42
	240–330	132.4	6.08×10^{5}	−106.6	125.3	109.5
	550–700	176.9	9.34×10^{7}	−185.7	161.5	183.4
	360-700	89.13	1.12×10^{7}	−45.75	49.89	40.68
$[Cd_2Cl_4H_2L(H_2O)_4]$	50-160	51.60	1.75×10^{10}	−76.97	28.86	40.67
	160-800	62.8	4.98×10^{9}	−45.22	59.95	71.22
$[UO_2(NO_3)_2H_2L(H_2O)_2].NO_3.2H_2O$	30–110	51.18	4.45×10^{7}	−56.14	50.46	50.66
	120–280	102.4	3.19×10^{12}	−95.28	99.43	91.86
	300–520	182.9	4.56×10^{11}	−166.7	128.4	152.3
	560–720	243.4	7.21×10^{7}	−203.2	195.8	192.6

3.9. Cyclic voltammetric study

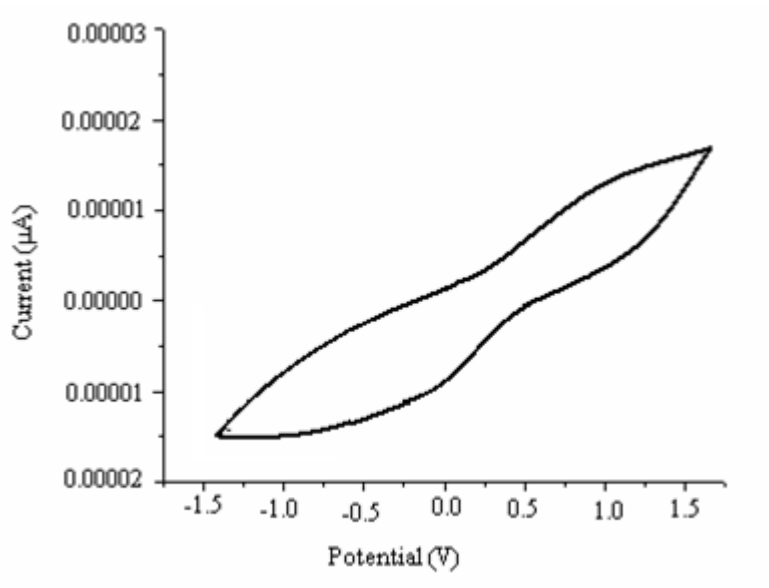

Figure 3. Cyclic voltammogram of Co(II) complex.

The cyclic voltammograms were recorded in acetonitrile solution at a scan rate of 100 mV s^{-1} in the potential range +2.0 to −2.0 V. The cyclic voltammogram of Co(II) complex (Figure 3) shows a

well defined redox process corresponding to the formation of the quasi-reversible Co(II)/Co(I) couple. The cathodic peak at −688 Mv versus Ag/AgCl and the associated anodic peak at −242 mV correspond to the Co(II)/Co(I) couple. The peak-to-peak separation (ΔEp = 448 mV) indicates quasi-reversible one electron transfer process. The redox property of Co(II) complex displayed electrochemically reversible Co(II)/Co(I) reduction peak at −705 mV and the associated oxidation peak at −259 mV corresponds to the Co(II)/Co(I) quasi-reversible process. The peak-to-peak separation (ΔEp) is 446 mV indicating the process to be quasi-reversible [32].

The electrochemistry of Ni(II) complex is similar to that of Ni(II) complex (Figure 4), anodic waves are seen at −811 and at −839 mV and the associated cathodic peaks at −693 and −679 mV respectively, corresponding to the formation of the quasi-reversible one-electron reduction Ni(II)/Ni(I) couple [33].

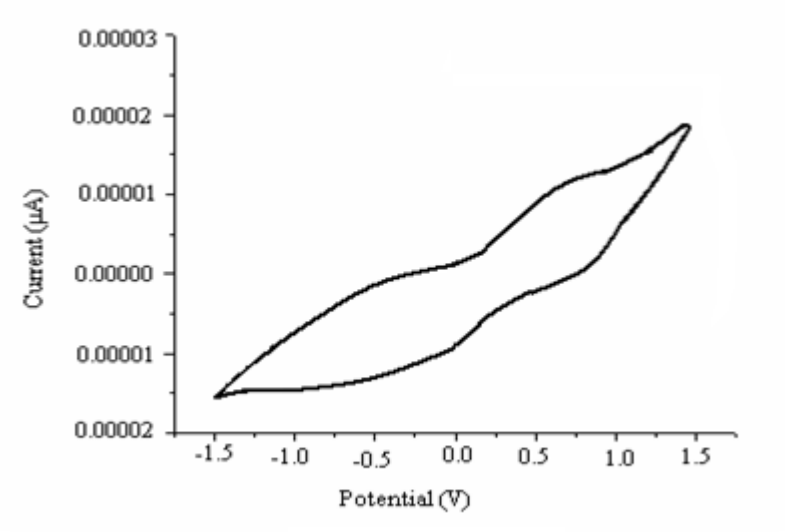

Figure 4. Cyclic voltammogram of Ni(II) complex.

The cyclic voltammogram of Cu(II) complex (Figure 5) (0.01 M) in MeCN (1.0 to –1.2 V potential range) shows a well-defined redox process corresponding to the formation of the Cu(II)/Cu(III) couple at E_{pa} = 0.22 V and the associated cathodic peak at E_{pc} = 0.18 V. This couple is found to be reversible with ΔE_p » 0.04 V and the ratio of anodic to cathodic peak currents (I_{pc}/I_{pa} = 1) corresponding to a simple one-electron process. The complex also shows a quasi-reversible peak in the negative region, characteristic of the Cu(II) → Cu(I) couple at E_{pc} = –0.66 V, with associated anodic peak at E_{pa} =–0.47 V for Cu(I) → Cu(II) oxidation [33]. The cyclic voltammogram of Zn(II) complex(Figure 6) (0.01 M) in MeCN solution in the absence of molecular oxygen at room temperature in 1.0 to –1.0 V potential range at scan rate 50 mVs^{-1} indicating quasi-reversible one-electron process. A noteworthy feature has been observed in the cyclic voltammogram of Zn(II) complex. During the forward scan it shows two cathodic reduction peaks, one at +0.45 V and another at –0.61 V which are attributed to reduction of Zn(II) → Zn(I) and Zn(I) → Zn(0) respectively [33].

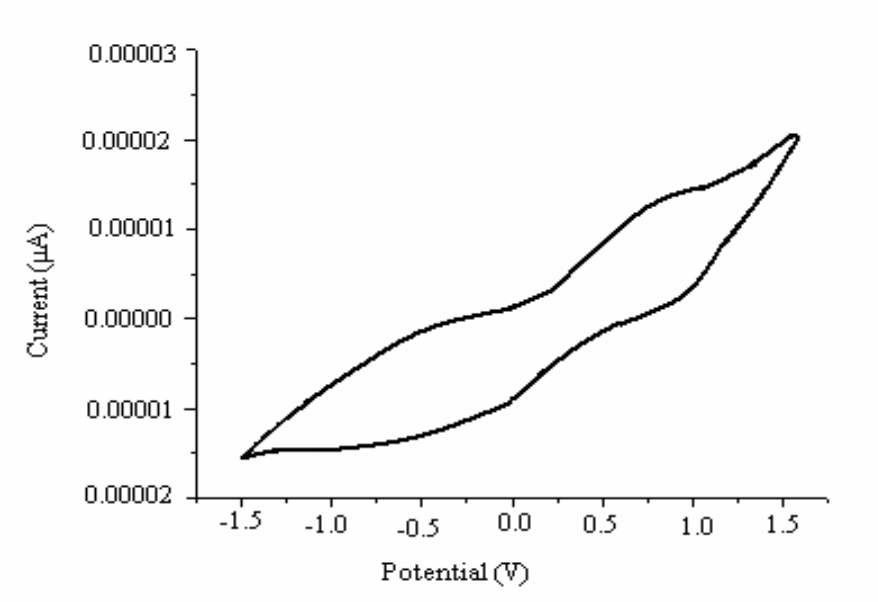

Figure 5. Cyclic voltammogram of Cu(II) complex.

During the reverse scan it shows two anodic oxidation peaks, one at –0.26 V and another at +0.62V which are attributed to oxidation of Zn(0) →Zn(I) and Zn(I) → Zn(II) respectively [33].

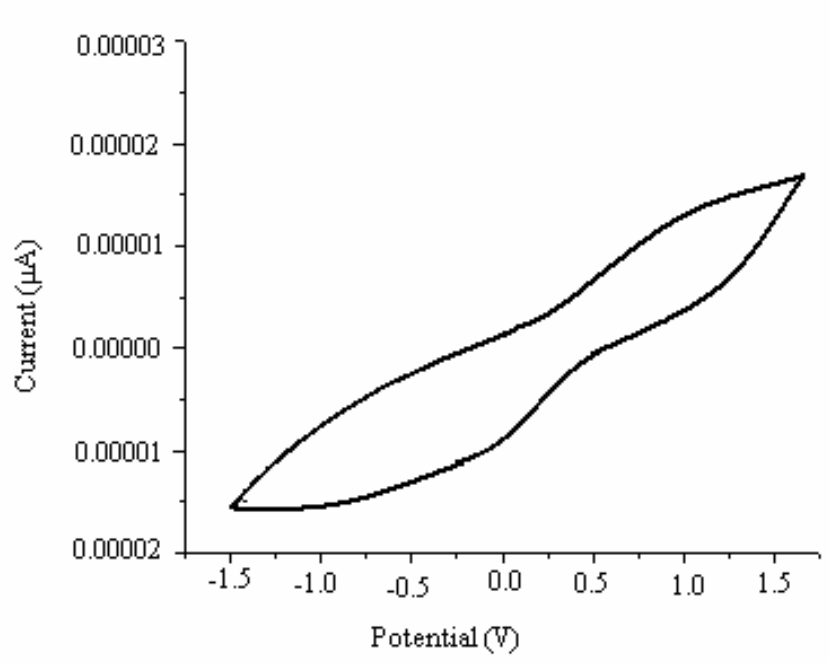

Figure 6. Cyclic voltammogram of Zn(II) complex.

Finally, the previous findings indicated that the coordination occurs through the sulfur of the thiophene group and the imine NH group to give the structures shown in Scheme 2.

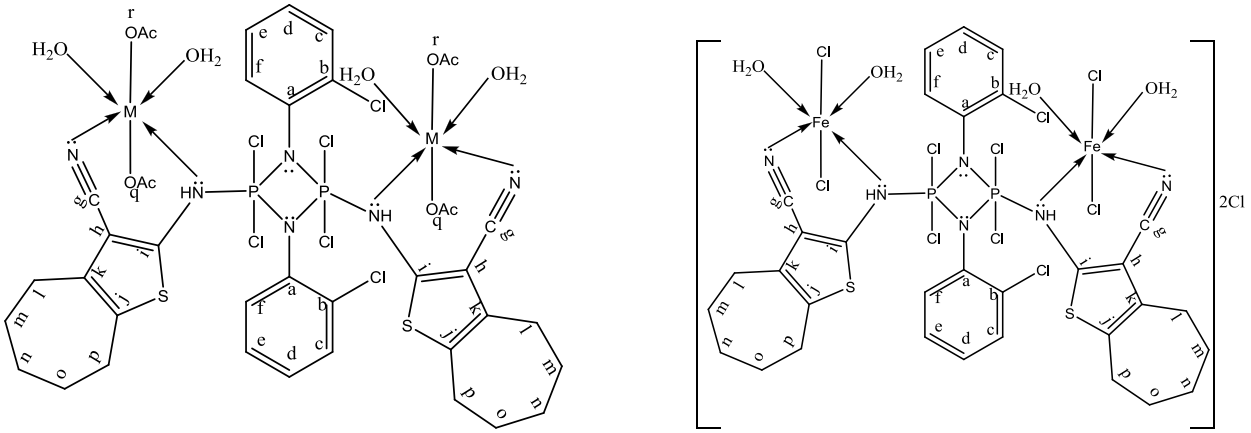

M = Mn(II), Co(II), Ni(II), Cu(II) and Zn(II)

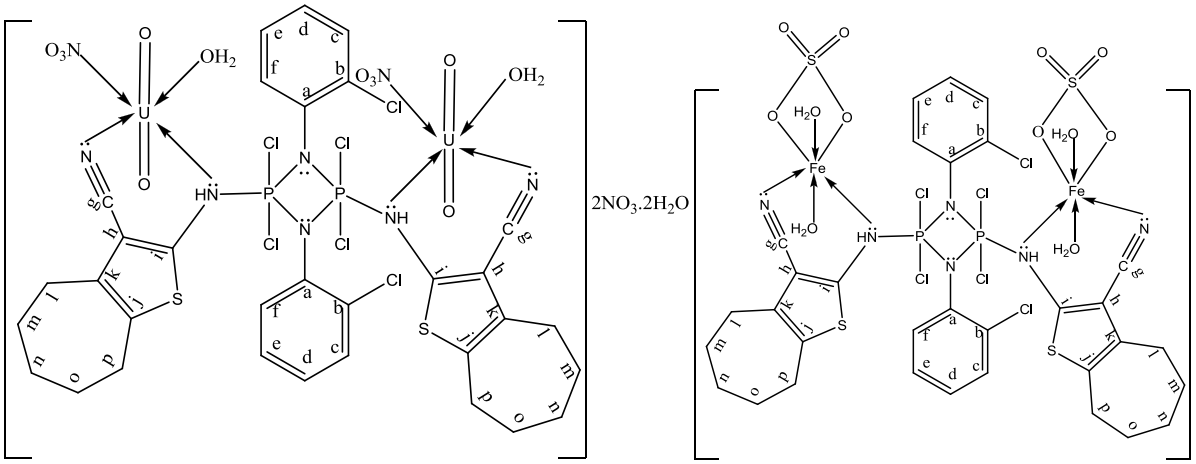

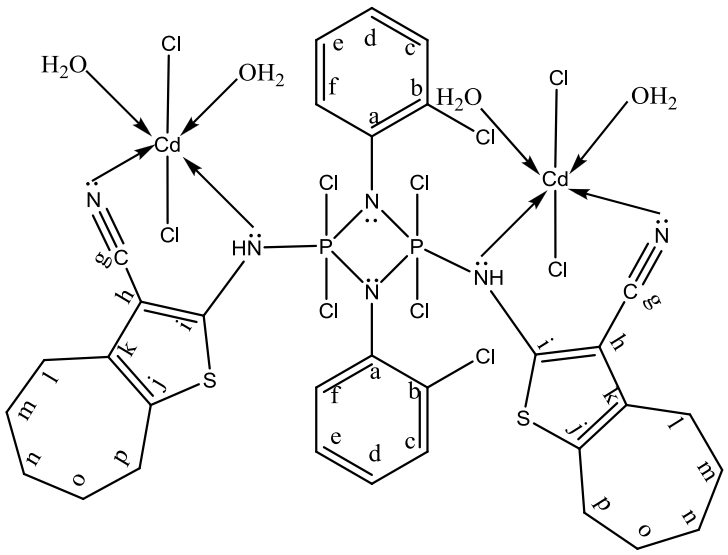

Scheme 2.

3.10. Biological activity

In testing the antibacterial activity of these compounds we used more than one test organism to increase the chance of detecting antibiotic principles in tested materials. The sensitivity of a

microorganism to antibiotics and other antimicrobial agents was determined by the assay plates which incubated at 28 °C for 2 days for yeasts and at 37 °C for 1 day for bacteria. The data showed that in some cases the ligand has a higher or similar antimicrobial activity than the selected standards (chloramphenicol and grisofluvine). Also, the presence of certain metal ions enhanced the antimicrobial activity of the ligand and in some cases a higher or similar activity than the selected standards were also showed (Table 6).

Table 6. Antimicrobial activity of H_2L and corresponding metal complexes

samples	Concentration (mg/mL)	Test organisms					
		Escherichia coli	*Salmonella typhi*	*Staphylococcus aureus*	*Bacillus subtillus*	*Aspergillus terreus*	*Aspergillus flavus*
H_2L	1	+++	+++	+++	+++	+++	+
	2.5	++	++	+++	+++	++	+
	5	+++	+++	+++	+++	++	+
$[Mn_2(OAc)_4\ H_2L(H_2O)_4]$	1				+++	++	+
	2.5	++	++	++	+++	++	+
	5	+++	+++	++	+++	++	+
$[(FeCl_2)_2\ H_2L(H_2O)_4].2Cl$	1	++	+	+	++	0	+
	2.5	++	++	++	+	0	+
	5	+++	+++	++	+++	++	+
$[FeSO_4)_2\ H_2L(H_2O)_4)]$	1	+	+	+	+++	++	0
	2.5	++	++	++	+++	++	++
	5	+++	+++	+++	+++	++	++
$[Co_2(OAc)_4\ H_2L(H_2O)_4]$	1	+	+	+		++	++
	2.5	++	++	++	++	++	+
	5	+++	+++	+++	+++	++	+
$[Ni_2(OAc)_4\ H_2L(H_2O)_4]$	1	++	++	+		++	+
	2.5	++	++	++	++	++	+
	5	+++	+++	+++	+++	+	+
$[Cu_2(OAc)_4\ H_2L(H_2O)_4]$	1	+	++	++	+	+	+
	2.5	++	++	++	++	+	+
	5	+++	+++	+++	+++	+	+
$[Zn_2(OAc)_4\ H_2L(H_2O)_4]$	1	+	+	+	+	+	0
	2.5	++	++	++	++	+	0
	5	+++	+++	+++	+++	+	+
$[Cd_2Cl_4\ H_2L(H_2O)_4]$	1	++	+	+	+	+	+
	2.5	+++	+++	+++	+++	+	+
	5	+++	+++	+++	+++	+	++
$[UO_2(NO_3)_2H_2L(H_2O)_2].NO_3.2H_2O$	1	++	+	+	+	+	+
	2.5	+++	++	++	+	+	+
	5	+++	+++	+++	+++	+	+
St.	1	++	+++	++	++	+++	+++
	2.5	+++	+++	++	+++	+++	+++
	5	+++	+++	+++	+++	+++	+++

St., reference standard; chloramphenicol was used as a standard antibacterial agent and grisofluvine was used as a standard antifungal agent. The test was done using the diffusion agar technique. Inhibition values = 0.1–0.5 cm beyond control = +; inhibition values = 0.6–1.0 cm beyond

control = ++; inhibition values = 1.1–1.5 cm beyond control = +++; inhibition values > 1.5 cm beyond control = ++++; 0 = not detected. Well diameter 1 cm (100µl of each conc. was tested).

References

1. P. Kommana and K. C. Kumara Swamy, *Inorg. Chem.*, 39 (2000) 4384.
2. K. P. Kumar, M. Chakravarty and K. C. *Z.* Kumara Swamy, *Anorg. Allg. Chem.*, 630 (2004) 2063.
3. M.S. Balakrishna, K. Ramaswamy and R.M. Abhyankar, *Organomet. Chem*. 560 (1998) 131.
4. C. Y. Park, F. V. Azzarello and A. J. Jacobson, *J. Mater. Chem.* 16 (2006) 3624.
5. N. Sari, S. Arslan, E. Logoglu and I. Sakiyan, *J. Sci.* 16 (2003) 283.
6. G.G. Mohamed and Z.H. Abd El-Wahwb, *J. Thermal Anal.* 73 (2003) 347.
7. W.G. Geary, Coord. *Chem. Rev.* 7 (1971) 81.
8. N.F. Curtis and Y.M. Curtis, *Inorg. Chem.* 4 (1964) 804.
9. L.K. Gupta, U. Bansal and S. Chandra, *Spectrochim. Acta A 66* (2007) 972.
10. C. Lodeiro, R. Bastida, E. Bertolo and A. Rodriguez, *Can. J. Chem.* 82 (2004) 437.
11. K. Nakamoto, Infrared and Raman Spectra of Inorganic and Coordination Compounds, third ed., Wiley Interscience, New York, 1978.
12. S. Chandra and Sangeetika, Spectrochim. Acta A 60 (2004) 2153.
13. P.J. Lucchesi and W.A. Glasson, J. Am. Chem. Soc. 78 (1956) 1347.
14. H.-J. Zhang, R.-H. Gou, L. Yan and R.D. Yang, Spectrochim. Acta A 66 (2007) 289.
15. I. M. Abd-Ellah, B. A. El-Sayed, M. A. El-Nawawy and A. M. A. Alaghaz *J. Phosphorus, Sulfur, and Silicon, and The Related Elements*, 177(2002) 2895.
16. A. M. A. Alaghaz and A. I. Hanafy, *J. Phosphorus, Sulfur, and Silicon, and The Related Elements*, 182 (2007) 1.
17. G. G. Mohamed, N. E. A. El-Gamel and F. A. Nour El-Dien, *Synth. React. Inorg. Met. Org. Chem.*, 31 (2) (2001) 347.
18. F. A. Cotton, G. Wilkinson, C. A. Murillo and M. Bochmann, *"Advanced Inorganic Chemistry"*, sixth ed., Wiley, New York, 1999.
19. A. B. P. Lever, *"Inorganic Electronic Spectroscopy"*, first ed., Elsevier Publishers, London/New York, pp. 267 (1968).
20. Z. M. Zaki, *Spectrosc. Lett.*, 31 (4) (1998) 757.
21. F. J. Barros-Garcña, A. Bernalte-Garcĭa, F. Luna-Giles, M. A. Maldonado-Rogado and E. Viñuelas-Zahĭnos, *Polyhedron* 24 (2005) 1125.
22. E. Rabinowitch, R. L. Belford, *"Spectroscopy and Photochemistry of Uranyl Compounds"*, Pergamon Press, New York, (1984).
23. N. N. Greenwood and T. C. Gibb, *"Mössbauer Spectroscopy"*, first ed., Champan and Hall Ltd. Publishers, London, (1971)pp. 248.
24. C.K. Jorgensen, *Acta Chim. Scand.* 10 (1956) 500.
25. R.S. Drago, *Physical Methods in Chemistry*. W. B. Saunders Company,1997, p. 530;
26. B.J. Hathaway and D.E. Billing, *Coord. Chem. Rev.* 6 (1970) 143.
27. B.J. Hathaway, J.N. Bradley, R.D. Gillard (Eds.), *Essays in Chemistry*, Academic Press, New York, 1971, p. 61.
28. B.J. Hathaway, R.J. Dudley and P. Nicholls, *J. Chem. Soc. A* (1968) 1845.
29. A. W. Coats and J. P. Redfern, *Nature* 201 (1964) 68.
30. V. Šatava and F. Škvara`, *J. Am. Ceram.* Soc. 52 (1969) 591.
31. S. Glasstone, Textbook of Physical Chemistry, second ed., Macmillan, Bombay, India, 1974.
32. S. P. Sovilj, G. Vučković, K. B. Babić-Samardžija, N. Matsumoto, V. M. Jovanović and J. Mroziński, *Synth. React. Inorg. Met. Org. Chem*. 29 (1999) 785-792.

33. R. Olar, M. Badea, D. Marinescu, M.-Carmen Chifiriuc, C. Bleotu, M. N. Grecu, E.-Elena Iorgulescu and V. Lazar, *Eur. J. Med. Chem.* 45 (2010) 3027–3034.